Enzyme-Free and Amplified Fluorescence DNA Detection Using Bimolecular Beacons

ARTICLE *in* ANALYTICAL CHEMISTRY · JUNE 2012

Impact Factor: 5.64 · DOI: 10.1021/ac3004727 · Source: PubMed

3 AUTHORS, INCLUDING:

Huang Jiahao
The Hong Kong University of Science and Tec…
19 PUBLICATIONS **183** CITATIONS
SEE PROFILE

Xuefen Su
The Chinese University of Hong Kong
27 PUBLICATIONS **322** CITATIONS
SEE PROFILE

analytical chemistry

Article

pubs.acs.org/ac

Graphene Oxide-Based Amplified Fluorescent Biosensor for Hg^{2+} Detection through Hybridization Chain Reactions

Jiahao Huang, Xiang Gao, Jingjing Jia, Jang-Kyo Kim, and Zhigang Li*

Department of Mechanical and Aerospace Engineering, The Hong Kong University of Science and Technology, Clear Water Bay, Kowloon, Hong Kong

ABSTRACT: We report a graphene oxide (GO)-based fluorescent sensor for Hg^{2+} detection in aqueous solutions by using hybridization chain reactions (HCRs). GO is used as an adsorption material for capturing single-stranded DNA and an efficient fluorescence quencher for reducing the background signal. In the detection strategy, two hairpin probes and a helper DNA are employed. Without Hg^{2+}, they are adsorbed by the GO and the fluorescence of one of the hairpin probes is quenched. In the presence of Hg^{2+}, the HCRs between the two hairpin probes are initiated by Hg^{2+} with the aid of the helper DNA through T-Hg^{2+}-T coordination chemistry. The double-stranded DNA products of the HCRs are released by the GO and the fluorescence is recovered. The detection limit of the sensing method is 0.3 nM, which is sufficiently sensitive for practical applications. The sensing system also exhibits high selectivity against other divalent metal ions, and the application of the sensor for drinking water shows that the proposed method works well for real samples.

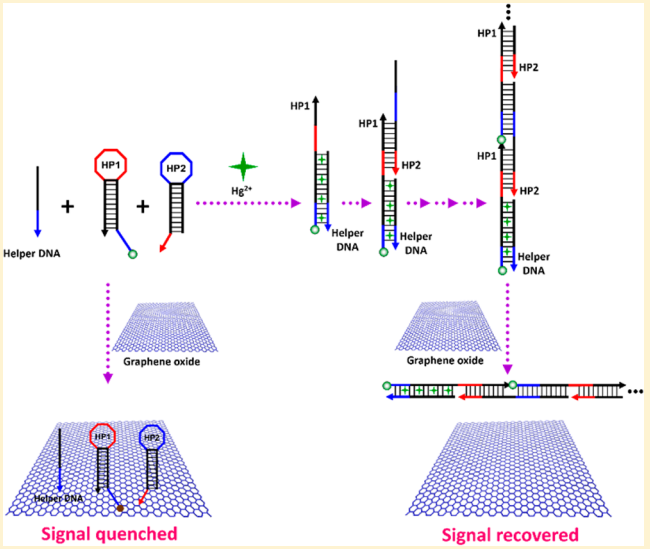

The emission of mercury and other toxic heavy metals has posed a challenge to the global plan of maintaining a sustainable environment. Water-soluble divalent mercuric ion (Hg^{2+}) is one of the most prevalent forms of mercury contamination, and the Hg^{2+} pollution of water sources is severe in many countries and regions. Mercury-mediated toxicity also has adverse effects on human health.[1,2] A small amount of mercury can cause damage to kidney, liver, and other organs. These environmental and health problems caused by Hg^{2+} have attracted great interest in the past decades to develop facile, sensitive, and reliable methods for efficient detection of Hg^{2+} in different media, including aqueous solutions.

Traditional techniques for Hg^{2+} analysis include inductively coupled plasma mass spectrometry,[3] atomic absorption spectroscopy,[4] and cold vapor atomic fluorescence spectroscopy.[5] Although these methods are very sensitive and accurate, they usually involve sophisticated instruments, time-consuming sample preparation steps, and a large amount of sample. Small organic molecule-based probes have also been developed.[6,7] These probes take advantage of their optical property changes upon binding to Hg^{2+}. They are simple and portable. However, poor selectivity and water solubility may limit their applications in aqueous environments.

To improve the selectivity for Hg^{2+} detection, oligonucleotides have been employed, on the basis of the finding that Hg^{2+} has high affinity for thymine−thymine (T-T) base pairs in DNA and can form stable T-Hg^{2+}-T structures.[8] Recently, different approaches have been developed that are based on this unique feature of coordination chemistry by using advanced materials, such as nucleic acid-related dyes,[9,10] conjugated polymers,[11,12] aggregation-induced emission probes,[13] magnetic particles,[14,15] silver nanoclusters,[16,17] silica nanoparticles,[18−20] gold nanoparticles,[21−25] carbon quantum dots,[26] carbon nanotubes,[27−30] and graphene oxide.[31,32] These methods have good selectivity, but many of their detection limits are above 10 nM, which may not be sufficiently sensitive for certain applications (e.g., the maximum allowable level of Hg^{2+} in drinking water is 10 nM, a standard set by the U.S. Environmental Protection Agency).[33]

Recently, some highly sensitive methods for Hg^{2+} detection have been proposed by employing catalytic DNAzyme[34−36] and quantum dots.[37−42] Unfortunately, most of them are not biocompatible. For example, the DNAzyme-based method[36] employs toxic uranium ions as a cofactor, and the quantum dots usually contain cadmium, selenium, and other toxic heavy metal elements. As biocompatible materials, protein enzymes have been widely used to amplify the response signal in DNA-based Hg^{2+} sensors. Strategies using horseradish peroxidase,[43,44] glucose oxidase,[45] exonuclease I,[46] exonuclease III,[47,48]

Received: January 16, 2014
Accepted: February 24, 2014
Published: February 24, 2014

   dx.doi.org/10.1021/ac500192r | *Anal. Chem.* 2014, 86, 3209−3215

Table 1. Hairpin DNA Probes and Other Oligonucleotides Used in Experiments.[a]

name	sequence (5′ to 3′)
HP1	FAM-*TTAACC***CACGCCGAATCCTAGACT**CAAAGT**AGTCTAGGATTCGGCGTG**
HP2	**AGTCTAGGATTCGGCGTG**GGTTAA**CACGCCGAATCCTAGACT***ACTTTG*
helper DNA1	TGTCTTGGTTTCGGCGTGGGTTTT
helper DNA2	AGACAAGGAAACGGCGAGGGAAAA

[a]Boldface type indicates stem sequences of hairpin DNA probes. Italic type in HP1 and HP2 shows sticky ends. Underlining represents mismatched sites.

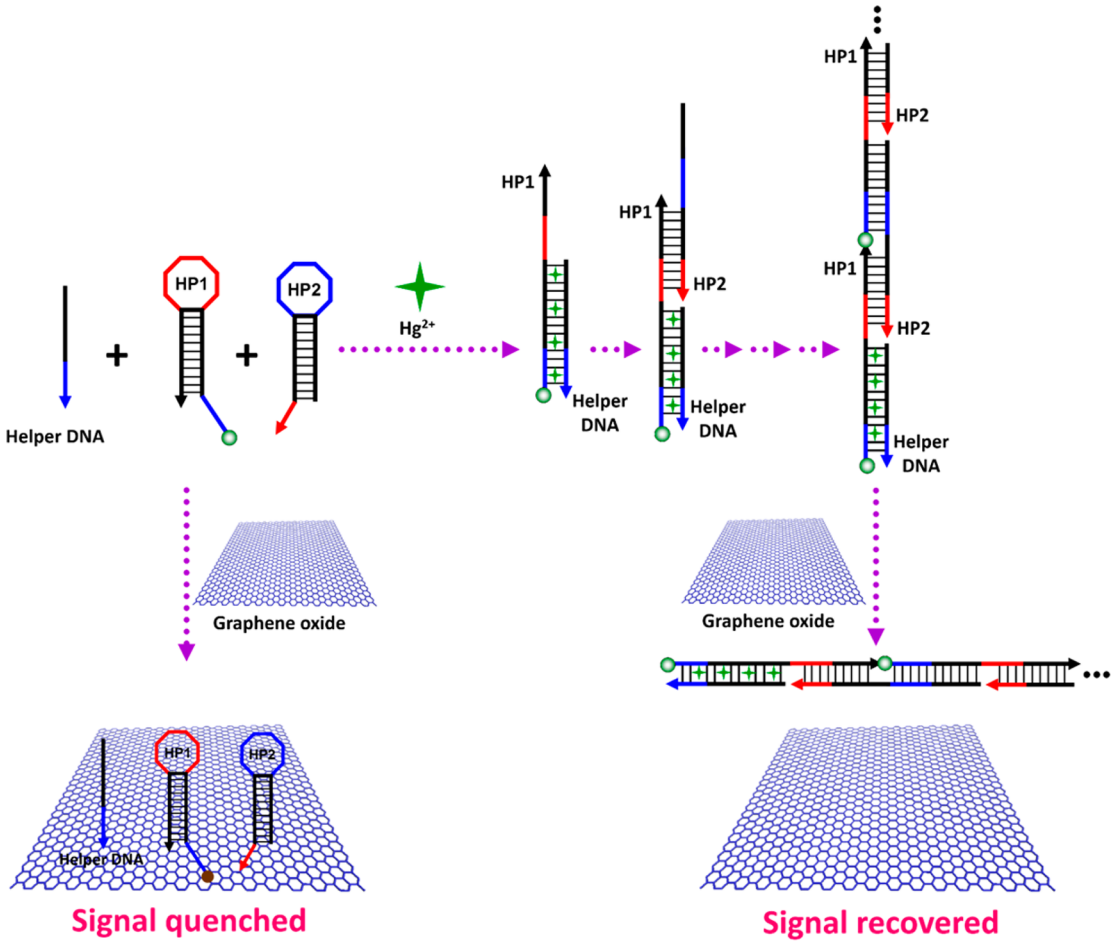

Figure 1. Schematic of the proposed detection mechanism (for clarity, pristine graphene is used to represent GO). In the absence of Hg^{2+}, GO absorbs the DNA probes (helper DNA, HP1, and HP2) through noncovalent interactions and quenches the fluorescence of HP1. However, in the presence of Hg^{2+}, the helper DNA opens HP1 due to the formation of stable T-Hg^{2+}-T structures and consequently induces continuous HP1-HP2 hybridizations, which cannot be adsorbed by GO, leading to the generation of amplified fluorescence.

polymerase,[49,50] and nicking endonuclease[51−53] have been reported with high sensitivities. Nevertheless, compared with other methods, protein enzymes make the detection relatively costly and complicated. Furthermore, the target, Hg^{2+}, may denature and affect the activity of the protein enzymes.

In this work, we report a "turn-on", sensitive, and selective method for Hg^{2+} detection in aqueous solutions by using graphene oxide (GO). In this sensing system, two specially designed hairpin DNA probes (HP1 and HP2) are employed. T-Hg^{2+}-T coordination chemistry is used to induce hybridization chain reactions (HCRs) of the hairpins with the aid of a helper DNA to amplify fluorescence generation. The HCR was first reported by Dirks and Pierce in 2004,[54] and has been widely used for enzyme-free amplified detection of DNA[55−58] and proteins.[59−61] However, HCRs have not been used for Hg^{2+} detection. GO is used as a quencher to turn off fluorescence emission in the absence of Hg^{2+}. GO is an attractive nanomaterial, which possesses distinct adsorption properties for single-stranded DNA (ssDNA) and double-stranded DNA (dsDNA).[62] Its fluorescence quenching ability for fluorophores is also superior to many other materials.[63,64] In addition, GO is a low-cost and environmentally friendly material. It also shows high water solubility and good biocompatibility. Therefore, the current detection method can overcome many of the disadvantages of the previous techniques.

EXPERIMENTAL SECTION

Materials. The hairpin probes (HP1 and HP2) and helper DNA1 and DNA2 were commercially synthesized by TaKaRa Bio Inc. (Dalian, China). Their sequences are listed in Table 1

dx.doi.org/10.1021/ac500192r | *Anal. Chem.* 2014, 86, 3209−3215

(helper DNA2 was used as a control here to demonstrate detection feasibility). HP1 was labeled with a fluorophore, FAM (fluorescein amidite). Both HP1 and HP2 have a stem of 18 base pairs (bp) and a loop of 6 nucleotides (nt) with an extra sticky tail of 6 nt (Figure 1). The sequences of HP1 and HP2 are complementary in a staggered configuration (Table 1), such that they will hybridize when HP1 is opened by helper DNA1. There are some T-T mismatches between the sequence of helper DNA1 and the stem and part of the loop sequence of HP1. However, some A-A mismatches are designed between the sequences of helper DNA2 and HP1. The monolayer GO sheets were synthesized through three successive intercalation steps: preintercalation of natural graphite, expansion at a high temperature, and oxidation by the modified Hummers method. The average lateral size was about 50−100 μm. Detailed information about GO fabrication can be found in our previous work.[65,66] $Hg(NO_3)_2$ was purchased from Sigma−Aldrich (St. Louis, MO). All other reagents were of analytical grade and were used without further purification or modification. All the solutions were prepared with water obtained from a NANOpure Diamond (Barnstead Int., Dubuque, IA) source.

Fluorescence Measurement. Fluorescence measurements were conducted on a F4500 fluorometer (Hitachi, Japan). According to the fluorescent properties of FAM labeled on HP1, the excitation and emission wavelengths were set at 496 and 525 nm. The slit width for both excitation and emission was set at 5 nm. To record the fluorescence emission spectra, samples were excited by a 496 nm light and scanned from 510 to 600 nm with a step of 1 nm. All the solutions (except that for understanding the effect of GO concentration) were 600 μL and prepared by mixing 100 nM HP1, 100 nM HP2, 500 nM helper DNA, and 100 μg/mL GO in the reaction buffer, which consisted of 50 mM $MgCl_2$ and 5 mM Tris-HCl with the pH value equal to 8.0. The mass ratio of HP1/HP2 to GO was around 0.0144, and that of helper DNA to GO was about 0.036. All the samples were incubated at 24 °C for at least 10 min before the experiments.

RESULTS AND DISCUSSION

Working Mechanism. The detection mechanism of the proposed sensor is illustrated in Figure 1. The system consists of three probes, including the helper DNA (DNA1 in Table 1), FAM-labeled HP1, and HP2. In the absence of Hg^{2+}, helper DNA is absorbed on the surface of GO due to the strong binding force between ssDNA and GO. Although HP1 and HP2 adopt the stem−loop structure, their sticky ends make them easily attach to the GO surface. Due to the super-quenching capability of GO, the fluorescence of FAM labeled on HP1 is expected to be very weak. In the presence of Hg^{2+}, however, Hg^{2+} will interact with the thymine bases in the helper DNA and the sticky tail of HP1 and form stable T-Hg^{2+}-T structures. This opens the hairpin structure of HP1 and exposes the rest of the sequence of HP1, which will bind with parts of HP2 and then open HP2. The exposed part of HP2 will then hybridize with the complementary sequences in HP1. Such HCRs will continue and generate a long chain of HP1−HP2−helper DNA−target complex. Theoretically, a small amount of Hg^{2+}, with the assistance of helper DNA, can trigger the formation of many such long chains. These long chains can easily detach from the GO, due to the weak binding force between long dsDNA and GO, and lead to the amplified fluorescence emission.

Effect of GO Concentration. The performance of GO plays a key role in the proposed detection strategy. The quenching ability of GO against its concentration was investigated first. Figure 2a shows the time response of the fluorescence intensity when the GO concentration was varied from 0 to 120 μg/mL with 100 nM HP1, 100 nM HP2, and 500 nM helper DNA1. It is seen that the fluorescence emission decreased with increasing GO concentration. Figure 2b depicts the quenching efficiency, which is defined as $(F_0 - F)/F_0$, where F and F_0 are the fluorescence intensities of the DNA solutions with and without GO, respectively. The signals were measured 20 min after GO was introduced. The quenching efficiency increased and then reached a plateau (larger than 90%) when the GO concentration was higher than 100 μg/mL, which was used in the experiments of this work. The greatly suppressed background signal is expected to help improve the sensitivity of the sensing method.

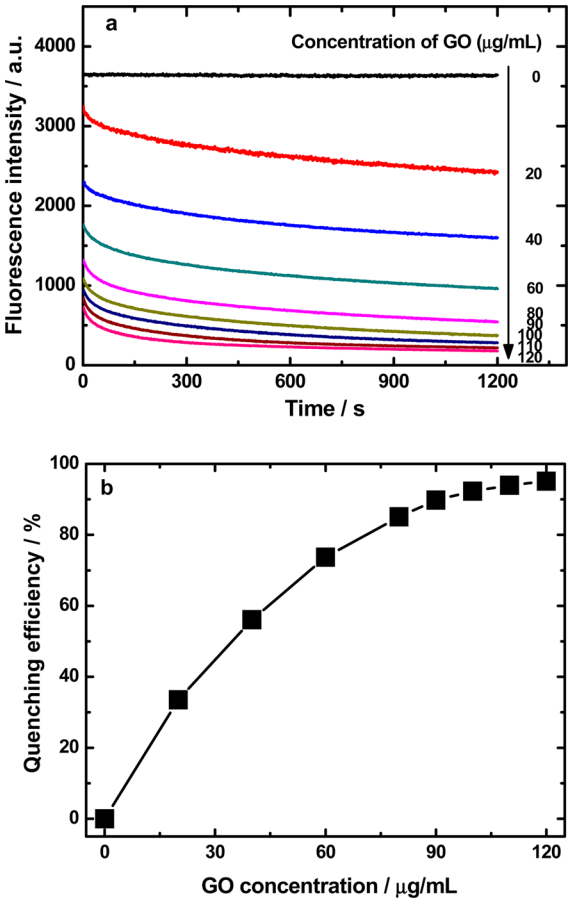

Figure 2. Effects of GO concentration on fluorescence response of the sensing system. (a) Time response of fluorescence intensity. (b) Quenching efficiency, $(F_0 - F)/F_0$, as a function of GO concentration. F and F_0 are fluorescence intensities of DNA solutions with and without GO, respectively.

Detection Feasibility. To test the feasibility of the proposed strategy, the fluorescence responses of different samples were studied. Figure 3 panels a and b depict fluorescence intensity and spectra, respectively. As illustrated in Figure 3a, the fluorescence intensity of the sample containing HP1, HP2, and helper DNA1 was about 3732 au. After 100 μg/mL GO was introduced into the sample, the fluorescence signal was significantly reduced to about 279.5 au after 20 min. In

dx.doi.org/10.1021/ac500192r | Anal. Chem. 2014, 86, 3209−3215

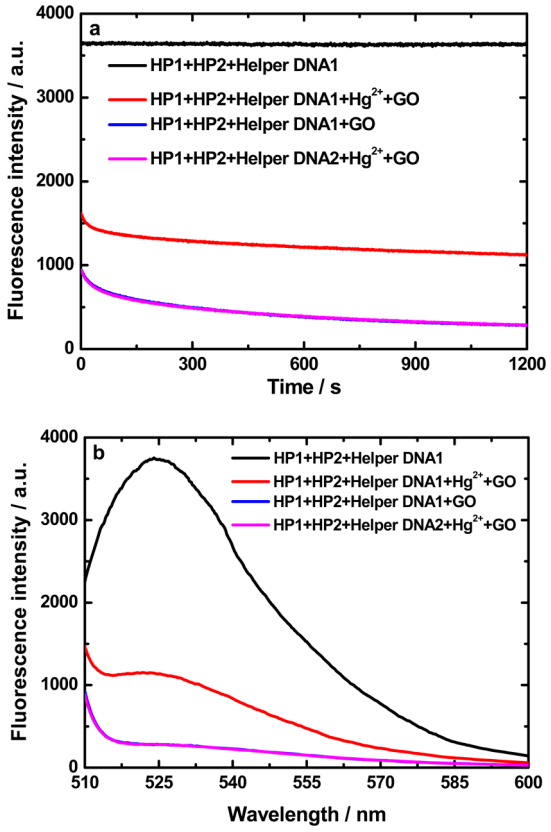

Figure 3. Fluorescence responses of different sensing systems: (a) kinetic studies and (b) fluorescence emission spectra. All the samples reacted at 24 °C for 1 h after the addition of 3 μM Hg^{2+}, and then 100 μg/mL GO was introduced.

contrast, in the presence of 3 μM Hg^{2+}, the response signal recovered and reached about 1137 au 20 min after GO was added into the solution. However, if helper DNA1 was replaced by helper DNA2, which could not trigger the HCRs, the response signal remained almost unchanged. This, together with the 4-fold fluorescence enhancement in the presence of Hg^{2+}, suggests that the HCRs were triggered by Hg^{2+} with the aid of helper DNA1 and the proposed detection principle in Figure 1 worked well. It is noted that GO was mixed with the solution after the target Hg^{2+} was introduced in the experiments. Such postmixing was found to have fast signal recovery kinetics compared with the premixing protocol, where $Hg^{2+}$was present after GO reacted with the HPs and helper DNA.[62] The postmixing strategy was also used in the sensitivity and selectivity analyses.

It is worth mentioning that many heavy metal ions, including Hg^{2+}, can act as fluorescence quenchers. Hence, the possibility of quenching the fluorescence by Hg^{2+} should be studied. Figure 4 shows the fluorescence intensity and quenching efficiency at different Hg^{2+} concentrations. It is seen that the quenching efficiency was less than 10% even when the Hg^{2+} concentration reached 1 μM. It should be mentioned that attention is usually paid to the low concentration range for highly sensitive sensors. Furthermore, this is a "turn-on" sensor, which is different from the "turn-off" methods[31,32] that may provide false indication caused by unexpected quenchers. Therefore, the slight quenching caused by Hg^{2+} has no significant effect on the proposed detection method.

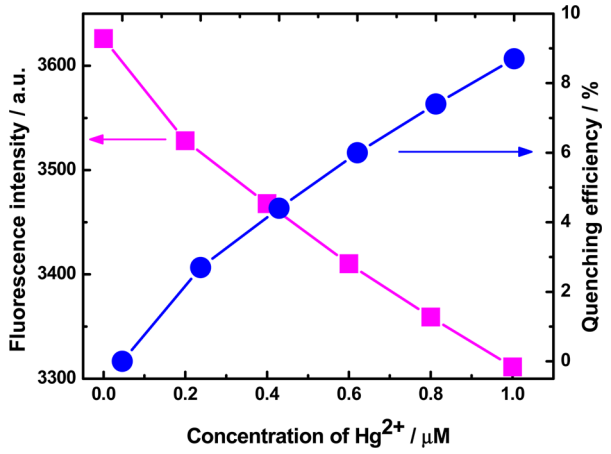

Figure 4. Fluorescence intensity and quenching efficiency, $(F_0 - F)/F_0$, as a function of Hg^{2+} concentration. F and F_0 are fluorescence intensities of DNA solutions with and without Hg^{2+}, respectively.

Detection Sensitivity. The sensitivity of the detection method was examined by changing the Hg^{2+} concentration. Figure 5a shows kinetic studies of the sensing system upon

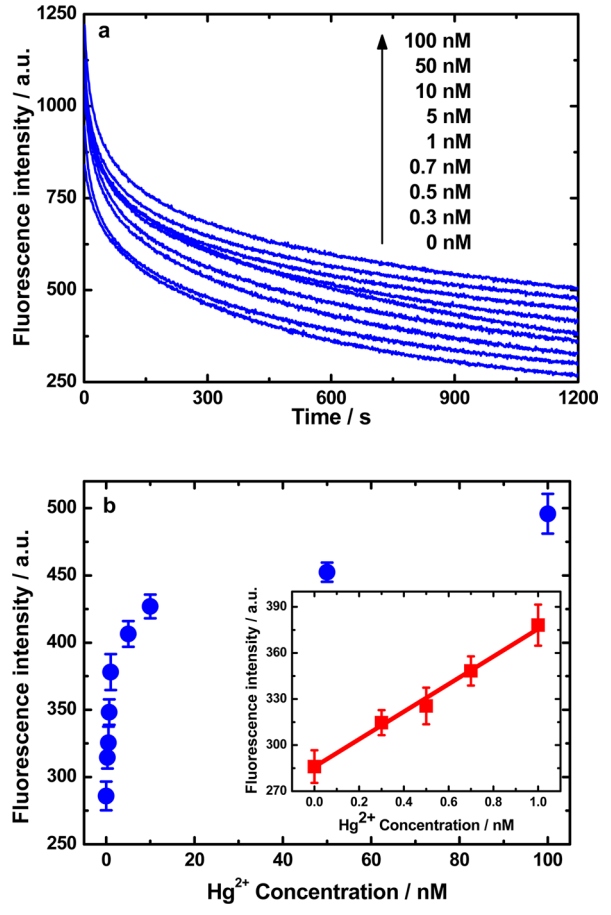

Figure 5. Fluorescence response of the sensing system at different Hg^{2+} concentrations. (a) Kinetic studies. (b) Relationship between fluorescence intensity and Hg^{2+} concentration. (Inset) Linear relationship in concentration range from 0 to 1.0 nM. All the samples reacted at 24 °C for 1 h after the addition of different concentrations of Hg^{2+} and then were quenched by 100 μg/mL GO for another 20 min.

dx.doi.org/10.1021/ac500192r | Anal. Chem. 2014, 86, 3209−3215

Table 2. Comparison of Different Hg^{2+} Detection Methods

ampl element[a]	method[b]	LOD[c]	analysis time	sensing mode	advantages	disadvantages	ref
conj polymers	F	5 μM	60 min	turn-on	high selectivity	poor sensitivity	11
Ag NCs	F	10 nM	8 h 15 min	turn-on	rapid, high selectivity	time-consuming assay procedures	16
silica NPs	F	20 nM	20 min	turn-on	rapid, low-cost, high selectivity	mediocre sensitivity	19
Au NPs	E	0.5 nM	135 min	turn-on	high sensitivity and selectivity	time-consuming sensor preparation	21
Au NPs	A	100 nM		turn-on	good selectivity	poor sensitivity	22
Au NPs	F	40 nM	30 min	turn-on	high selectivity	mediocre sensitivity	23
Au NPs	A	3 μM	5 min	turn-on	instrument-free	poor sensitivity	24
carbon QDs	F	203 nM		turn-off	cost-effective, high selectivity	poor reliability and sensitivity	26
CNTs	E	16.3 fM	55 min	turn-on	high sensitivity and selectivity	time-consuming sensor preparation	28
CNTs	F	14.5 nM	20 min	turn-on	simple, rapid, good selectivity	mediocre sensitivity	30
GO	F	0.92 nM	5 min	turn-off	low-cost, high sensitivity and selectivity	poor reliability	31
GO	F	0.5 nM	10 min	turn-off	high sensitivity and selectivity	poor reliability	32
DNAzyme	A	9.7 pM	155 min	turn-on	high sensitivity and selectivity	relatively long analysis time	34
QDs	F	10 nM		turn-off	universal, good multiplexity	poor reliability	37
QDs/Au NPs	F	2 nM	10 min	turn-off	high sensitivity and selectivity	poor reliability, time-consuming sample pretreatment	39
QDs/nicking endo	F	0.8 nM	140 min	turn-on	high sensitivity	complicated	40
QDs	P	1.5 nM	30 min	turn-off	high sensitivity and selectivity	poor reliability	41
HRP/Au NPs	E	52 pM	45 min	turn-on	high sensitivity and selectivity	time-consuming sensor preparation	43
glucose oxidase	E	100 pM	30 min	turn-on	high sensitivity	time-consuming sensor preparation	45
exo I	F	15 nM	90 min	turn-on	simple and low-cost	mediocre sensitivity	46
exo III/CNTs/Ag NCs	F	33 pM	160 min	turn-on	high sensitivity and selectivity	complicated system and high cost	47
exo III	E	0.2 nM	70 min	turn-on	high sensitivity and selectivity	time-consuming sensor preparation	48
polymerase/nicking endo	F	2.0 pM	60 min	turn-on	high sensitivity and selectivity	complicated system and high cost	53
GO	F	0.3 nM	140 min	turn-on	simple, high sensitivity and selectivity	relatively time-consuming	this work

[a]Ag NCs, silver nanoclusters; Au NPs, gold nanoparticles; QDs, quantum dots; CNTs, carbon nanotubes; GO, graphene oxide; HRP, horseradish peroxidase; endo, endonuclease; exo, exonuclease. [b]F, fluorescence; E, electrochemistry; A, absorbance; P, phosphorescence. [c]LOD, limit of detection.

addition of GO after incubation with Hg^{2+} for 1 h. It is found that the fluorescence intensity increased with increasing Hg^{2+} concentration at any instantaneous time. The dependence of fluorescence intensity on Hg^{2+} concentration is plotted in Figure 5b. The response signal was proportional to the Hg^{2+} concentration in the range from 0 to 1.0 nM, and the limit of detection (LOD) was experimentally determined as 0.3 nM, which was the lowest concentration that could generate fluorescence emission distinguishable from the background signal. It is close to the theoretical limit of 0.36 nM, which is the value of $3\sigma/S$ (σ is the standard deviation of the background signal and S is the slope of the fluorescence–target concentration line shown in the inset of Figure 5b). This LOD is 1–2 orders of magnitude lower than that of gold nanoparticle-based colorimetric assays[22−24] and enzyme-assisted amplification methods.[46,51] It is sufficiently sensitive for practical applications, such as Hg^{2+} detection in drinking water. To compare with other methods, Table 2 summarizes some key properties of other DNA-based sensing systems for Hg^{2+} detection.

Detection Selectivity. The selectivity of the sensing method was also evaluated by monitoring the fluorescence response when the sensing system was challenged with other divalent metal ions, including Ca^{2+}, Mg^{2+}, Zn^{2+}, Cu^{2+}, Fe^{2+}, Mn^{2+}, Ni^{2+}, and Co^{2+}. As shown in Figure 6, 3 μM Hg^{2+} produced a significantly higher fluorescence signal compared with that caused by other metal ions at 10 μM. Figure 6 also reveals that the coexistence of Hg^{2+} and other metal ions did not affect detection by the sensor. This is an essential requirement for practical applications because it is very

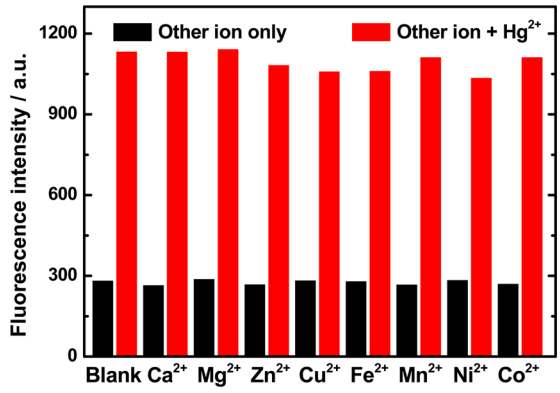

Figure 6. Selectivity of the sensing method against other metal ions. Concentrations of Hg^{2+} and other metal ions were 3 and 10 μM, respectively. Black bars represent the responses of the sensing system challenged with a specific metal ion. Red bars show the responses of the sensing system in the presence of 3 μM Hg^{2+} and 10 μM corresponding metal ions. All the samples reacted for 1 h after addition of different metal ions and then were quenched by 100 μg/mL GO for another 20 min.

dx.doi.org/10.1021/ac500192r | Anal. Chem. 2014, 86, 3209−3215

common that real samples contain different metal ions. The high selectivity of the sensing method is due to the fact that T-T mismatch shows high affinity for Hg^{2+} against many other metal ions and the binding force for T-Hg^{2+}-T is reported to be even stronger than that of the Watson−Crick A-T base pair.[67]

Practical Application. To test the sensing method, recovery experiments for drinking water with different Hg^{2+} concentrations were carried out. The drinking water samples were obtained from the tap in our laboratory. The signal generated from the drinking water samples was about 278.6 au 20 min after GO was added, suggesting that Hg^{2+} concentration was far below 10 nM in the drinking water (Figure 5a). Fortification solutions of different Hg^{2+} concentrations were then added to the samples, and Hg^{2+} levels were evaluated. The results are summarized in Table 3. It is found that the proposed sensor could accurately determine the Hg^{2+} concentration in drinking water.

Table 3. Recovery Experiments of Hg^{2+} in Drinking Water Samples[a]

sample	Hg^{2+} added (nM)	Hg^{2+} detected (nM)	recovery (%)
1	0.4	0.41 ± 0.03	101.5 ± 7.3
2	0.6	0.58 ± 0.04	96.9 ± 7.5
3	0.8	0.79 ± 0.06	99.1 ± 7.1

[a]Mean values and standard deviations were obtained from three independent experiments.

CONCLUSIONS

An HCR- and GO-based fluorescent sensor has been developed for the "turn-on" detection of Hg^{2+} in aqueous solutions. In the sensing system, the target, Hg^{2+}, induced the formation of long duplex chains through T-Hg^{2+}-T coordination chemistry and amplified the fluorescence emission. The HCRs guaranteed high sensitivity of the method. GO was employed as an excellent fluorescence quencher to lower the background signal and help strengthen the detection sensitivity further. GO also functioned as the signal controller by selectively adsorbing ssDNA and liberating long dsDNA products. The detection limit of the proposed method was experimentally obtained as 0.3 nM. Experiments for drinking water demonstrated that the detection method was applicable for detection of Hg^{2+} in real samples.

AUTHOR INFORMATION

Corresponding Author

*E-mail mezli@ust.hk.

Notes

The authors declare no competing financial interest.

ACKNOWLEDGMENTS

This work was supported by the Research Grants Council of the Hong Kong Special Administrative Region under Grant 615710.

REFERENCES

(1) Nolan, E. M.; Lippard, S. J. *Chem. Rev.* **2008**, *108*, 3443−3480.
(2) Zahir, F.; Rizwi, S. J.; Haq, S. K.; Khan, R. H. *Environ. Toxicol. Pharmacol.* **2005**, *20*, 351−360.
(3) Bings, N. H.; Bogaerts, A.; Broekaert, J. A. C. *Anal. Chem.* **2006**, *78*, 3917−3946.
(4) Ghaedi, M.; Fathi, M. R.; Shokrollahi, A.; Shajarat, F. *Anal. Lett.* **2006**, *39*, 1171−1185.
(5) Rea, A. W.; Keeler, G. J. *Biogeochemistry* **1998**, *40*, 115−123.
(6) Coronado, E.; Galán-Mascarós, J. R.; Martí-Gastaldo, C.; Palomares, E.; Durrant, J. R.; Vilar, R.; Gratzel, M.; Nazeeruddin, M. K. *J. Am. Chem. Soc.* **2005**, *127*, 12351−12356.
(7) Kim, H. N.; Lee, M. H.; Kim, H. J.; Kim, J. S.; Yoon, J. *Chem. Soc. Rev.* **2008**, *37*, 1465−1472.
(8) Ono, A.; Togashi, H. *Angew. Chem., Int. Ed.* **2004**, *43*, 4300−4302.
(9) Chiang, C. K.; Huang, C. C.; Liu, C. W.; Chang, H. T. *Anal. Chem.* **2008**, *80*, 3716−3721.
(10) Wang, J.; Liu, B. *Chem. Commun.* **2008**, 4759−4761.
(11) Lee, J.; Jun, H.; Kim, J. *Adv. Mater.* **2009**, *21*, 3674−3677.
(12) Liu, X. F.; Tang, Y. L.; Wang, L. H.; Zhang, J.; Song, S. P.; Fan, C. H.; Wang, S. *Adv. Mater.* **2007**, *19*, 1471−1474.
(13) Xu, J. P.; Song, Z. G.; Fang, Y.; Mei, J.; Jia, L.; Qin, A. J.; Sun, J. Z.; Ji, J.; Tang, B. Z. *Analyst* **2010**, *135*, 3002−3007.
(14) Li, Q.; Zhou, X. M.; Xing, D. *Biosens. Bioelectron.* **2010**, *26*, 859−862.
(15) Zheng, J.; Nie, Y. H.; Hu, Y. P.; Li, J. S.; Li, Y. H.; Jiang, Y.; Yang, R. H. *Chem. Commun.* **2013**, *49*, 6915−6917.
(16) Deng, L.; Zhou, Z. X.; Li, J.; Li, T.; Dong, S. J. *Chem. Commun.* **2011**, *47*, 11065−11067.
(17) MacLean, J. L.; Morishita, K.; Liu, J. W. *Biosens. Bioelectron.* **2013**, *48*, 82−86.
(18) He, D. G.; He, X. X.; Wang, K. M.; Zhao, Y. X.; Zou, Z. *Langmuir* **2013**, *29*, 5896−5904.
(19) Zhang, Y. F.; Yuan, Q.; Chen, T.; Zhang, X. B.; Chen, Y.; Tan, W. H. *Anal. Chem.* **2012**, *84*, 1956−1962.
(20) Zhu, X.; Chen, L. F.; Lin, Z. Y.; Qiu, B.; Chen, G. N. *Chem. Commun.* **2010**, *46*, 3149−3151.
(21) Kong, R. M.; Zhang, X. B.; Zhang, L. L.; Jin, X. Y.; Huan, S. Y.; Shen, G. L.; Yu, R. Q. *Chem. Commun.* **2009**, 5933−5935.
(22) Lee, J. S.; Han, M. S.; Mirkin, C. A. *Angew. Chem., Int. Ed.* **2007**, *46*, 4093−4096.
(23) Wang, H.; Wang, Y. X.; Jin, J. Y.; Yang, R. H. *Anal. Chem.* **2008**, *80*, 9021−9028.
(24) Xue, X. J.; Wang, F.; Liu, X. G. *J. Am. Chem. Soc.* **2008**, *130*, 3244−3245.
(25) Ye, B. C.; Yin, B. C. *Angew. Chem., Int. Ed.* **2008**, *47*, 8386−8389.
(26) Zhang, R. Z.; Chen, W. *Biosens. Bioelectron.* **2014**, *55*, 83−90.
(27) Guo, L. Q.; Yin, N.; Nie, D. D.; Gan, J. R.; Li, M. L.; Fu, F. F.; Chen, G. N. *Analyst* **2011**, *136*, 1632−1636.
(28) Guo, L. Q.; Yin, N.; Nie, D. D.; Gan, J. R.; Li, M. L.; Fu, F. F.; Chen, G. N. *Chem. Commun.* **2011**, *47*, 10665−10667.
(29) Niu, S. Y.; Li, Q. Y.; Ren, R.; Hu, K. C. *Anal. Lett.* **2010**, *43*, 2432−2439.
(30) Zhang, L. B.; Tao, L.; Li, B. L.; Jing, L.; Wang, E. K. *Chem. Commun.* **2010**, *46*, 1476−1478.
(31) Li, M.; Zhou, X. J.; Ding, W. Q.; Guo, S. W.; Wu, N. Q. *Biosens. Bioelectron.* **2013**, *41*, 889−893.
(32) Zhang, J. R.; Huang, W. T.; Xie, W. Y.; Wen, T.; Luo, H. Q.; Li, N. B. *Analyst* **2012**, *137*, 3300−3305.
(33) U.S. Environmental Protection Agency. EPA-452/R-05-003; U.S. Government Printing Office, Washington, DC, 2005.
(34) Hao, Y. L.; Guo, Q. Q.; Wu, H. Y.; Guo, L. Q.; Zhong, L. S.; Wang, J.; Lin, T. R.; Fu, F. F.; Chen, G. N. *Biosens. Bioelectron.* **2014**, *52*, 261−264.
(35) Jia, S. M.; Liu, X. F.; Li, P.; Kong, D. M.; Shen, H. X. *Biosens. Bioelectron.* **2011**, *27*, 148−152.
(36) Liu, J. W.; Lu, Y. *Angew. Chem., Int. Ed.* **2007**, *46*, 7587−7590.
(37) Freeman, P.; Finder, T.; Willner, I. *Angew. Chem., Int. Ed.* **2008**, *48*, 7818−7821.
(38) Huang, D. W.; Niu, C. G.; Wang, X. Y.; Lv, X. X.; Zeng, G. M. *Anal. Chem.* **2013**, *85*, 1164−1170.
(39) Li, M.; Wang, Q. Y.; Shi, X. D.; Hornak, L. A.; Wu, N. Q. *Anal. Chem.* **2011**, *83*, 7061−7065.

(40) Ma, J.; Chen, Y. H.; Hou, Z.; Jiang, W.; Wang, L. *Biosens. Bioelectron.* **2013**, *43*, 84−87.
(41) Xie, W. Y.; Huang, W. T.; Luo, H. Q.; Li, N. B. *Analyst* **2012**, *137*, 4651−4653.
(42) Zhang, J. N.; Tian, J. N.; He, Y. L.; Zhao, Y. C.; Zhao, S. L. *Chem. Commun.* **2014**, *50*, 2049−2051.
(43) Wang, G. F.; Huang, H.; Zhang, X. J.; Wang, L. *Biosens. Bioelectron.* **2012**, *35*, 108−114.
(44) Zhang, Z. P.; Tang, A. M.; Liao, S. Z.; Chen, P. F.; Wu, Z. Y.; Shen, G. L.; Yu, R. Q. *Biosens. Bioelectron.* **2011**, *26*, 3320−3324.
(45) Mor-Piperberg, G.; Tel-Vered, R.; Elbaz, J.; Willner, I. *J. Am. Chem. Soc.* **2010**, *132*, 6878−6879.
(46) Yuan, M.; Zhu, Y. G.; Lou, X. H.; Chen, C.; Wei, G.; Lan, M. B.; Zhao, J. L. *Biosens. Bioelectron.* **2012**, *31*, 330−336.
(47) Wang, G. F.; Xu, G.; Zhu, Y. H.; Zhang, X. J. *Chem. Commun.* **2014**, *50*, 747−750.
(48) Xuan, F.; Luo, X. T.; Hsing, I. M. *Anal. Chem.* **2013**, *85*, 4586−4593.
(49) Yin, J. J.; He, X. X.; Jia, X. K.; Wang, K. M.; Xu, F. Z. *Analyst* **2013**, *138*, 2350−2356.
(50) Zhu, X.; Zhou, X. M.; Xing, D. *Biosens. Bioelectron.* **2011**, *26*, 2666−2669.
(51) Li, D.; Wieckowska, A.; Willner, I. *Angew. Chem., Int. Ed.* **2008**, *47*, 3927−3931.
(52) Shi, L.; Chu, Z. Y.; Liu, Y.; Jin, W. Q.; Chen, X. J. *Biosens. Bioelectron.* **2014**, *54*, 165−170.
(53) Zhu, G. C.; Li, Y.; Zhang, C. Y. *Chem. Commun.* **2014**, *50*, 572−574.
(54) Dirks, R. M.; Pierce, N. A. *Proc. Natl. Acad. Sci. U.S.A.* **2004**, *101*, 15275−15278.
(55) Chen, Y.; Xu, J.; Su, J.; Xiang, Y.; Yuan, R.; Chai, Y. Q. *Anal. Chem.* **2012**, *84*, 7750−7755.
(56) Huang, J.; Wu, Y. R.; Chen, Y.; Zhu, Z.; Yang, X. H.; Yang, C. J.; Wang, K. M.; Tan, W. H. *Angew. Chem., Int. Ed.* **2011**, *50*, 401−404.
(57) Liu, P.; Yang, X. H.; Sun, S.; Wang, Q.; Wang, K. M.; Huang, J.; Liu, J. B.; He, L. L. *Anal. Chem.* **2013**, *85*, 7689−7695.
(58) Wang, F. A.; Elbaz, J.; Orbach, R.; Magen, N.; Willner, I. *J. Am. Chem. Soc.* **2011**, *133*, 17149−17151.
(59) Xu, Q. F.; Zhu, G. C.; Zhang, C. Y. *Anal. Chem.* **2013**, *85*, 6915−6921.
(60) Zhang, B.; Liu, B Q.; Tang, D. P.; Niessner, R.; Chen, G. N.; Knopp, D. *Anal. Chem.* **2012**, *84*, 5392−5399.
(61) Zhou, J.; Xu, M. D.; Tang, D. P.; Gao, Z. Q.; Tang, J.; Chen, G. N. *Chem. Commun.* **2012**, *48*, 12207−12209.
(62) He, S. J.; Song, B.; Li, D.; Zhu, C. F.; Qi, W. P.; Wen, Y. Q.; Wang, L. H.; Song, S. P.; Fang, H. P.; Fan, C. H. *Adv. Funct. Mater.* **2010**, *20*, 453−459.
(63) Huang, J. H.; Zheng, Q. B.; Kim, J. K.; Li, Z. G. *Biosens. Bioelectron.* **2013**, *43*, 379−383.
(64) Li, F.; Pei, H.; Wang, L. H.; Lu, J. X.; Gao, J. M.; Jiang, B. W.; Zhao, X. C.; Fan, C. H. *Adv. Funct. Mater.* **2013**, *23*, 4140−4148.
(65) Zheng, Q. B.; Ip, W. H.; Lin, X. Y.; Yousefi, N.; Yeung, K. K.; Li, Z. G.; Kim, J. K. *ACS Nano* **2011**, *5*, 6039−6051.
(66) Zheng, Q. B.; Zhang, B.; Lin, X. Y.; Shen, X.; Yousefi, N.; Huang, Z. D.; Li, Z. G.; Kim, J. K. *J. Mater. Chem.* **2012**, *22*, 25072−25082.
(67) Zhu, Z. Q.; Su, Y. Y.; Li, J.; Li, D.; Zhang, J.; Song, S. P.; Zhao, Y.; Li, G. X.; Fan, C. H. *Anal. Chem.* **2009**, *81*, 7660−7666.